Complex band structure of flexural waves in 2-D metamaterial Kirchhoff-Love plates with shunted piezo-patches

E.J.P. Miranda Jr. [1,2,3], **J.M.C. Dos Santos** [3]
[1] Federal Institute of Maranhão, IFMA-EIB-DE,
Rua Afonso Pena, 174, CEP 65010-030, São Luís, MA, Brazil

[2] Federal Institute of Maranhão, IFMA-PPGEM,
Avenida Getúlio Vargas, 4, CEP 65030-005, São Luís, MA, Brazil

[3] University of Campinas, UNICAMP-FEM-DMC,
Rua Mendeleyev, 200, CEP 13083-970, Campinas, SP, Brazil
e-mail: **edson.jansen@ifma.edu.br**

Abstract
The wave propagation in a 2-D mechanical metamaterial Kirchhoff-Love plate with periodic arrays of shunted piezo-patches is investigated. This piezoelectric mechanical metamaterial thin plate is capable of filtering the propagation of flexural waves over a specified range of frequency, called band gaps. The real and complex band structures are obtained by the improved plane wave expansion (IPWE) and extended plane wave expansion (EPWE) methods, respectively. The Bragg-type and locally resonant band gaps are both opened up. The shunt circuits influence significantly the propagating and the evanescent modes. The results can be used for elastic wave attenuation using 2-D piezoelectric periodic structures.

1 Introduction

Recently, the piezoelectric shunt damping combined with the concept of periodic structures originated the piezoelectric mechanical metamaterials (PMMs). In terms of wave attenuation, the advantage of using PMMs is the formation of both Bragg-type and locally resonant band gaps [1]. These forbidden bands are regions of frequency where there are only evanescent waves [2, 3]. In addition, the 1-D [4, 5] and 2-D [1, 6, 7] PMMs have been extensively studied by experimental techniques and numerically.

Chen [1] obtained the band structure of 2-D acoustic metamaterials with shunting circuits by using the finite element (FE) method with COMSOL. He observed an attenuation zone around the band gap location, in which the wave propagation decayed strongly.

Xiao *et al.* [7] designed an adaptive hybrid laminate acoustic metamaterial composed of a carbon-fiber-reinforced polymer and a periodic array of piezoelectric shunting patches attached to the laminate. They demonstrated by using FE approach that the lightweight adaptive hybrid laminate metamaterial with the shunting circuits can remarkably suppress wave propagation compared to the un-shunted case. Moreover, they discussed the effects of the laminate's parameters as well as the shunting circuits on the band gap's location and bandwidth. They also introduced a negative capacitance shunting circuit into the piezoelectric patches in order to enlarge the band gap width.

In this investigation, the band structures are numerically obtained by the improved plane wave expansion (IPWE) [8, 2, 3, 9] and extended plane wave expansion (EPWE) [10, 2, 3] methods. First, the cases of open and short circuits are studied. Next, two types of closed electrical circuits are considered, *i.e.*, resistive and resonant circuits.

2 Piezoelectric metamaterial plate modeling

Figure 1 sketches the top (a) and front (b) views of the 2-D PMM unit cell. The piezoelectric patches with shunting circuits connected in parallel are illustrated in (b) for the cases of resistive ($Z^{SU} = R$) and resonant ($Z^{SU} = R + i\omega L$) circuits, where $i = \sqrt{-1}$, ω is the angular frequency, Z^{SU} is the electrical impedance, R is the resistance and L is the inductance of the electrical circuit. In Fig. 1 (c), it is shown the first irreducible Brillouin zone (FIBZ) [11] of the 2-D PMM for a square lattice, where the FIBZ high-symmetry points are Γ $(0, 0)$, X $(\pi/a, 0)$ and M $(\pi/a, \pi/a)$ and a is the lattice parameter.

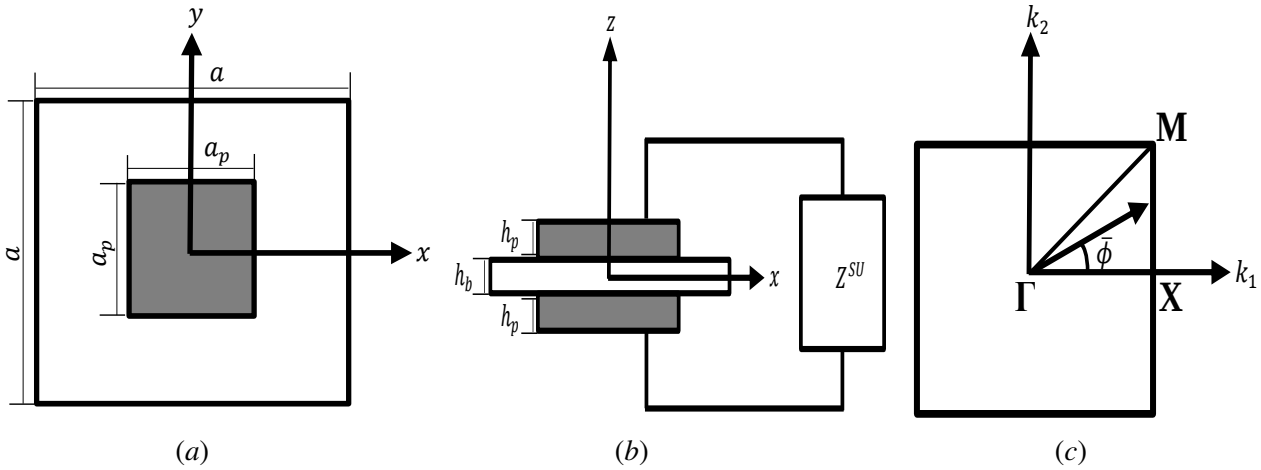

(a) (b) (c)

Figure 1: Top (a) and front (b) views of the 2-D PMM unit cell. First irreducible Brillouin zone of the 2-D PMM for a square lattice.

The IPWE, $\omega(\mathbf{k})$, is used to compute the propagating modes, whereas the EPWE, $\mathbf{k}(\omega)$, can be used to obtain both propagating and evanescent modes of the band structure, where $\mathbf{k}$ is the Bloch wave vector (also known as wave number). It should be highlighted that the IPWE method has higher convergence than the traditional plane wave expansion (PWE) approach [8]. Furthermore, the band structure computed by IPWE shows a considerably lower computational cost [9], since it is a semi-analytical approach and it is not necessary to consider a large number of degrees-of-freedom as with other methods. The IPWE and EPWE formulations will be derived in a future publication. However, some fundamental issues associated with these approaches can be found in [12, 13].

The Kirchhoff-Love [14, 15] thin plate theory is used to model the 2-D PMMs with periodic arrays of shunted piezo-patches with a square cross section area (Fig. 1 (a)). The evanescent modes obtained by the EPWE are related to the wave attenuation in the unit cell, since it is defined as $\Im\{\mathbf{k}\}a$ [3]. In this paper, the media are isotropic and only flexural (*i.e.*, out-of-plane) modes are considered.

3 Simulated examples

The physical parameters [7, 16] of the plate (b) and the piezoelectric patches (p) are listed in Table 1. It should be pointed out that the plate and piezoelectric patch loss factors are not considered. Moreover, the dynamic equivalent modulus and Poisson's ratio of piezo-patches can be obtained by using [7]:

$$E_p(\omega) = \frac{h_p[1 + i\omega Z^{SU}(\omega)C_p^{\varepsilon}]}{h_p s_{11}^E[1 + i\omega Z^{SU}(\omega)C_p^{\varepsilon}] - i\omega Z^{SU}(\omega)d_{31}^2 A_s}, \tag{1}$$

$$\nu_p(\omega) = -\frac{s_{12}^E[1 + i\omega Z^{SU}(\omega)C_p^{\varepsilon}] - i\omega Z^{SU}(\omega)d_{31}^2 A_s h_p^{-1}}{s_{11}^E[1 + i\omega Z^{SU}(\omega)C_p^{\varepsilon}] - i\omega Z^{SU}(\omega)d_{31}^2 A_s h_p^{-1}}. \tag{2}$$

Table 1: Geometry and material properties of the plate (b) and piezoelectric patches (PZT-5H) (p).

Geometry/Property	**Value**
Lattice parameter (a)	0.06 m
Piezoelectric patch length (a_p)	0.03 m
Plate thickness (h_b)	0.0016 m
Piezoelectric patch thickness (h_p)	0.0002 m
Mass density (ρ_b, ρ_p)	1.6×10^3 kg/m^3, 7.5×10^3 kg/m^3
Young's modulus (E_b, $E_p(\omega)$)	181×10^9 N/m^2, Eq. 1
Poisson's ratio (ν_b, $\nu_p(\omega)$)	0.28, Eq. 2
Compliance coefficient at constant electric field (s_{11}^E)	16.5×10^{-12} 1/Pa
Compliance coefficient at constant electric field (s_{12}^E)	-4.78 $\times 10^{-12}$ 1/Pa
Piezoelectric strain constant (d_{31})	-2.74 $\times 10^{-10}$ C/N
Dielectric constant (ε_{33}^σ)	$3400\varepsilon_0$
Electromechanical coupling coefficient (k_{31})	0.35
Electrical capacitance of the piezo at constant strain (C_p^ε)	118.87×10^{-9} F

Hereafter, the model assurance criterion (MAC) [17] is used to estimate the correlation among wave mode shapes for the EPWE. Furthermore, for IPWE and EPWE calculations and comparison, 49 plane waves are regarded, in order to reduce the computational time (*i.e.*, the Fourier series convergence is not verified) and the band structure is analyzed only on the ΓX direction, *i.e.*, $\bar{\phi} = 0$.

Figure 2 shows the complex band structure of the 2-D PMM plate for the case of open circuit ($Z^{SU} \to \infty$).

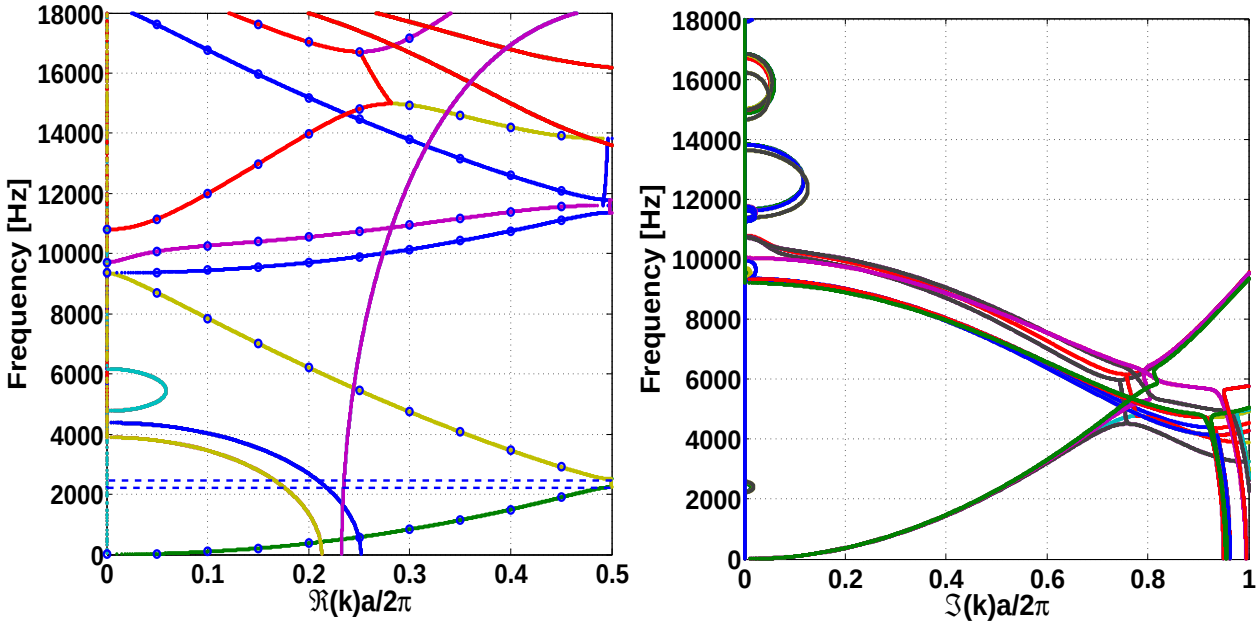

(*a*) (*b*)

Figure 2: Complex band structure of the 2-D PMM plate with open circuit ($Z^{SU} \to \infty$) computed by (a) IPWE (blue circles) and $(a-b)$ EPWE (points) methods.

In Fig. 2 (a), one can note that the IPWE (blue circles) can identify only the propagating modes. The evanescent modes with complex wave numbers are obtained by the EPWE (points). A good agreement between the IPWE and EPWE is observed (Fig. 2 (a)). Note that some modes in Fig. 2 (a) cannot be found by the IPWE, since they are complex. For EPWE calculation, a $\Delta f = 1$ Hz is regarded. The band gap in

Fig. 2 (a) (blue dashed rectangle) is created only by Bragg scattering along ΓX direction (partial band gap), since there is no electrical resonance. This Bragg-type band gap is opened up between 2239-2513 Hz and can be directly observed by the propagating modes from IPWE. The unit cell wave attenuation inside this band gap can be seen in Fig. 2 (b). Moreover, there are also other regions of wave attenuation in higher frequencies that are shown in Fig. 2 (b). It should be underlined that the best strategy to identify a complete band gap is to identify whether all Bloch waves are evanescent within it [12].

Figure 3 shows the complex band structure for the case of short ($Z^{SU} = 0$) circuit. Two partial band gaps (Fig. 3 (a)) are created between 1948-2150 Hz and 7823-8127 Hz. A good agreement between the IPWE and EPWE (Fig. 3 (a)) is observed, similar to the open circuit case (Fig. 2 (a)).

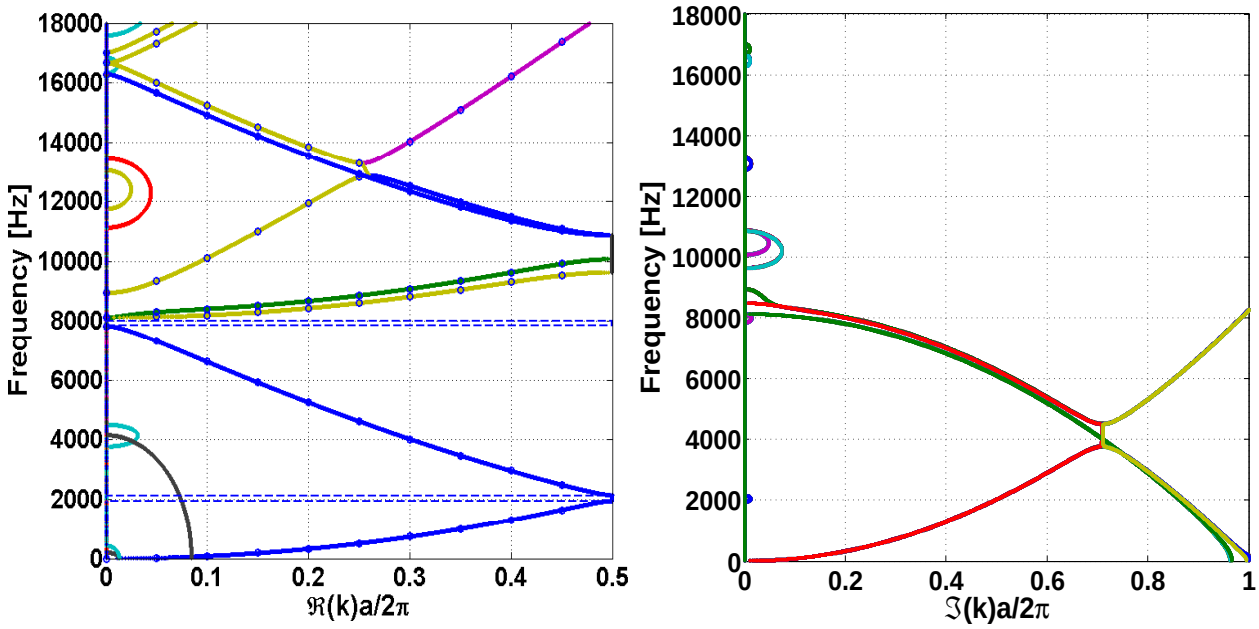

(a) (b)

Figure 3: Complex band structure of the 2-D PMM plate with short circuit ($Z^{SU} = 0$) computed by (a) IPWE (blue circles) and $(a-b)$ EPWE (points) methods.

Figure 4 illustrates the complex band structure for the case of resistive ($R = 50\ \Omega$) circuit.

This band structure behavior is similar to the short circuit case (Fig. 3), however, the resistor slightly increases the total piezoelectric loss factor (Fig. 4).

It should be underlined that the IPWE cannot be directly used to compute the band structures for the cases of closed circuit (resistive and resonant circuits), since there are some properties depending on the frequency (Eqs. 1 and 2). However, an iterative algorithm can be designed to obtain the band gap structure due to the dependence of elastic constants [18].

Figure 5 presents the complex band structure for the case of resonant circuit ($f_T = 768.786$ Hz), where f_T is the resonance of the electrical circuit. The locally resonant band gap can be observed in Fig. 5 around the resonant frequency. The resonance is easily identified considering for instance only the first four modes (see Fig. 6). Moreover, this resonant frequency can be computed by [7]:

$$f_T = \frac{1}{2\pi\sqrt{L(C_p^{\varepsilon} - C_h)}}, \tag{3}$$

where

$$C_h = \frac{d_{31}^2 A_s / h_p}{s_{11}^E - \dfrac{12(s_{11}^E - s_{12}^E)^2 \left\| \begin{bmatrix} \bar{D}_{11} & \bar{D}_{12} & \bar{D}_{16} \\ \bar{D}_{12} & \bar{D}_{22} & \bar{D}_{26} \\ \bar{D}_{16} & \bar{D}_{26} & \bar{D}_{66} \end{bmatrix} \right\|}{(1-a_p^2/a^2)[(h+2h_p)^3 - h^3] + 24(s_{11}^E - s_{12}^E) \left\| \begin{bmatrix} \bar{D}_{11} & \bar{D}_{12} & \bar{D}_{16} \\ \bar{D}_{12} & \bar{D}_{22} & \bar{D}_{26} \\ \bar{D}_{16} & \bar{D}_{26} & \bar{D}_{66} \end{bmatrix} \right\|}}. \tag{4}$$

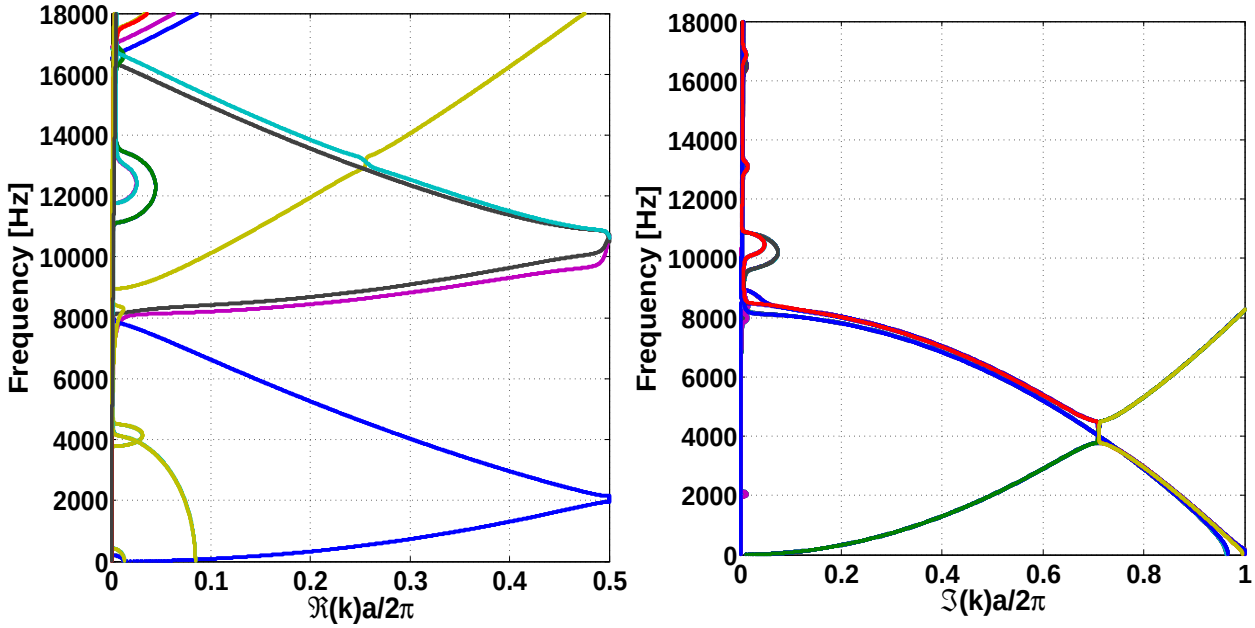

(*a*) (*b*)

Figure 4: Complex band structure of the 2-D PMM plate with resistive circuit ($R = 50\ \Omega$) computed by EPWE.

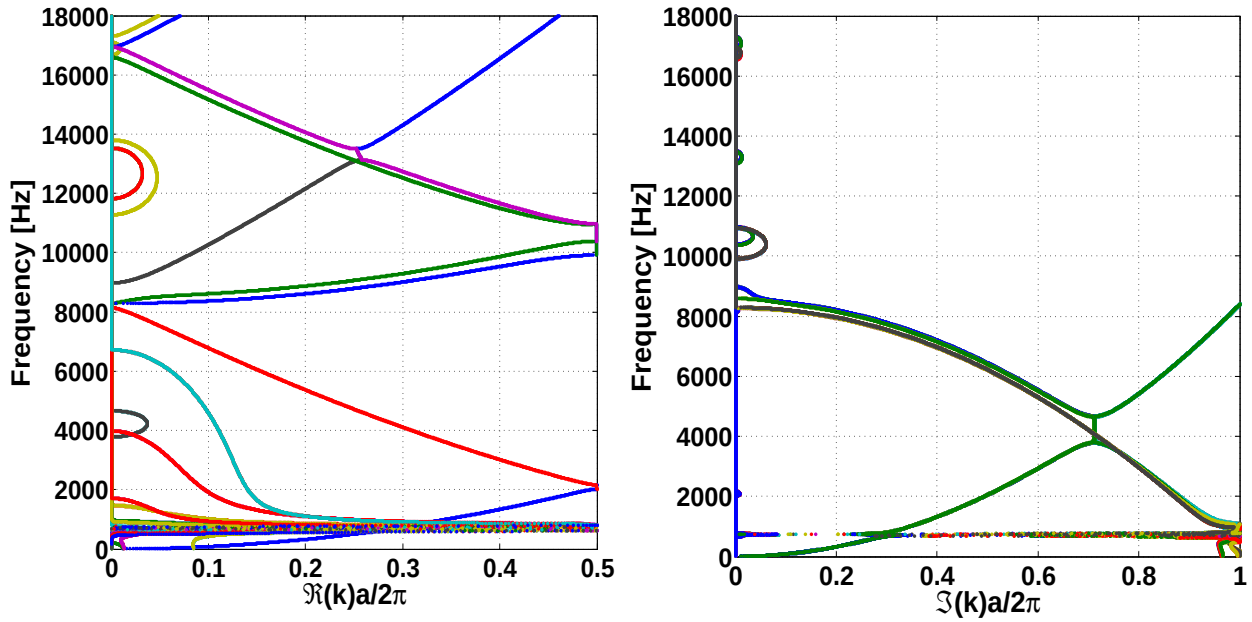

(*a*) (*b*)

Figure 5: Complex band structure of the 2-D PMM plate with resonant circuit ($f_T = 768.786$ Hz) computed by EPWE.

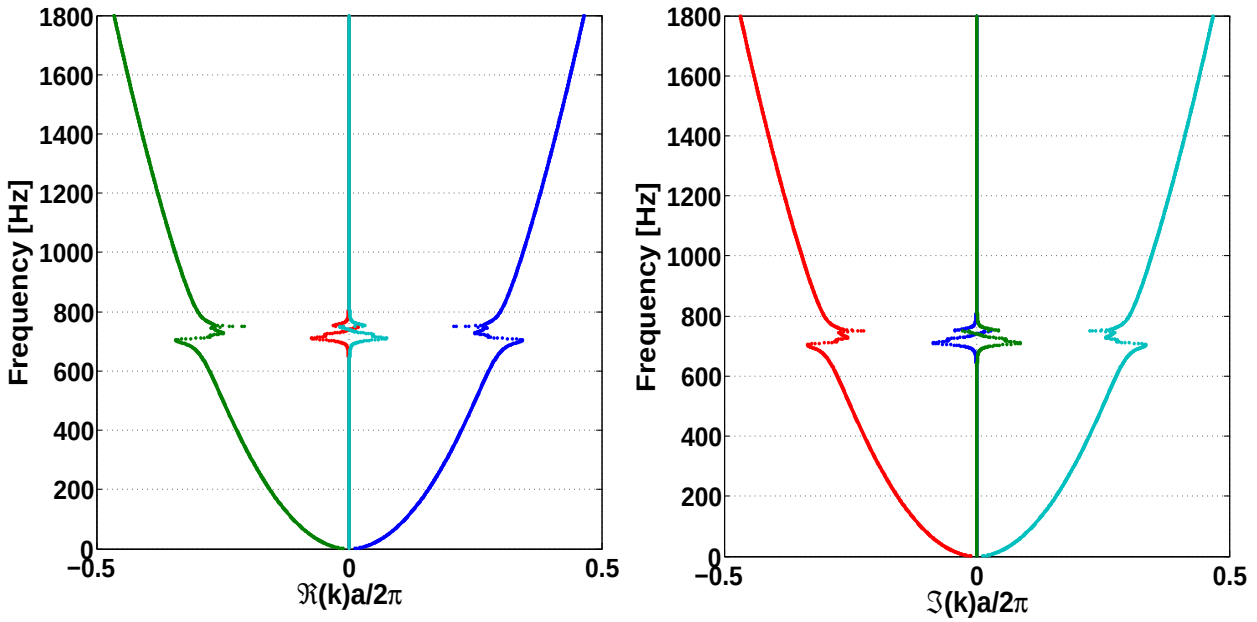

(*a*) (*b*)

Figure 6: Complex band structure zoom (only the first four modes) around the locally resonant band gap of the 2-D PMM plate with a resonant circuit ($f_T = 768.786$ Hz) computed by the EPWE.

4 Conclusions

The complex band structures of a 2-D mechanical metamaterial thin plate with periodic arrays of shunted piezo-patches are investigated. These band structures computed by IPWE and EPWE approaches show good agreement. The Bragg-type band gaps are first observed for the open and short circuits. Next, the resistive and resonant circuits are studied and the locally resonant band gap is opened up for the resonant case. The

results can be used for elastic wave attenuation using 2-D piezoelectric periodic structures.

Acknowledgments

The authors gratefully acknowledge the support of the Federal Institute of Maranhão (IFMA), Brazilian funding agencies CAPES (Finance Code 001), CNPq (Grant Reference Numbers 313620/2018 and 151311/2020-0), FAPEMA (Grant Reference Numbers 02558/21, 02559/21, 00680/22 and 07733/22) and FAPESP (Grant Reference Number 2018/15894-0).

References

[1] S. Chen, "Wave propagation in acoustic metamaterials with resonantly shunted cross-shape piezos," *Journal of Intelligent Material Systems*, vol. 29, no. 13, pp. 2744–2753, 2018.

[2] E. J. P. Miranda Jr., E. D. Nobrega, A. H. R. Ferreira, and J. M. C. Dos Santos, "Flexural wave band gaps in a multi-resonator elastic metamaterial plate using Kirchhoff-Love theory," *Mechanical Systems and Signal Processing*, vol. 116, pp. 480–504, 2019.

[3] E. J. P. Miranda Jr., E. D. Nobrega, S. F. Rodrigues, C. Aranas Jr., and J. M. C. Dos Santos, "Wave attenuation in elastic metamaterial thick plates: Analytical, numerical and experimental investigations," *International Journal of Solids and Structures*, vol. 204-205, pp. 138–152, 2020.

[4] C. Sugino, S. Leadenham, M. Ruzzene, and A. Erturk, "An investigation of electroelastic bandgap formation in locally resonant piezoelectric metastructures," *Smart Materials and Structures*, vol. 26, no. 055029, 2017.

[5] E. J. P. Miranda Jr., E. D. Nobrega, L. P. R. Oliveira, and J. M. C. Dos Santos, "Elastic wave propagation in metamaterial rods with periodic shunted piezo-patches," in *INTER-NOISE and NOISE-CON Congress and Conference Proceedings*, Washington, D.C., USA, 2021, pp. 4303–4311.

[6] A. Aghakhani, M. M. Gozum, and I. Basdogan, "Modal analysis of finite-size piezoelectric metamaterial plates," *Journal of Physics D: Applied Physics*, vol. 53, no. 505340, 2020.

[7] X. Xiao, Z. C. He, E. Li, B. Zhou, and X. K. Li, "A lightweight adaptive hybrid laminate metamaterial with higher design freedom for wave attenuation," *Composite Structures*, vol. 243, no. 112230, 2020.

[8] Y. Cao, Z. Hou, and Y. Liu, "Convergence problem of plane-wave expansion method for phononic crystals," *Physics Letters A*, vol. 327, no. 247-253, 2004.

[9] V. F. Dal Poggetto and A. L. Serpa, "Elastic wave band gaps in a three-dimensional periodic metamaterial using the plane wave expansion method," *International Journal of Mechanical Sciences*, vol. 184, p. 105841, 2020.

[10] Y.-C. Hsue, A. J. Freeman, and B.-Y. Gu, "Extended plane-wave expansion method in three-dimensional anisotropic photonic crystals," *Physical Review B*, vol. 72, no. 195118, 2018.

[11] L. Brillouin, *Wave Propagation in Periodic Structures*. New York: Dover Publications, 1946.

[12] V. Laude, Y. Achaoui, S. Benchabane, and A. Khelif, "Evanescent Bloch waves and the complex band structure of phononic crystals," *Physical Review B*, vol. 80, p. 092301, 2009.

[13] E. J. P. Miranda Jr., S. F. Rodrigues, C. Aranas Jr., and J. M. C. Dos Santos, "Plane wave expansion and extended plane wave expansion formulations for Mindlin-Reissner elastic metamaterial thick plates," *Journal of Mathematical Analysis and Applications*, vol. 505, no. 2, p. 125503, 2022.

[14] G. Kirchhoff, "Über das gleichgewicht und die bewegung einer elastischen scheibe," *Journal für die reine and angewandtle Mathematik*, vol. 40, pp. 51–88, 1850.

[15] A. E. H. Love, "The small free vibrations and deformation of a thin elastic shell," *Philosophical Transactions of the Royal Society*, vol. 179, pp. 491–546, 1888.

[16] J. J. Hollkamp, "Multimodal passive vibration suppression with piezoelectric materials and resonant shunts," *Journal of Intelligent Material Systems and Structures*, vol. 5, no. 49-57, 1994.

[17] J.-M. Mencik, "On the low- and mid-frequency forced response of elastic structures using wave finite elements with one-dimensional propagation," *Computers and Structures*, vol. 88, pp. 674–689, 2010.

[18] Y. P. Zhao and P. J. Wei, "The band gap of 1D viscoelastic phononic crystal," *Computational Materials Science*, vol. 46, no. 3, pp. 603–606, 2009.